

6.5 kV SiC Power Devices with Improved Blocking Characteristics against Process Deviations

Junki Jung^{1,2}, Ogyun Seok^{3,*}, In Ho Kang², Hyoung Woo Kim^{2,*}, Wook Bahng², and Ho-Jun Lee¹

Abstract—Edge termination structures that are insensitive to process deviations were investigated to obtain 6.5 kV SiC power devices with stable blocking characteristics. Edge terminations were designed and verified by a TCAD simulation in consideration of undesirable surface charge states and variation of the implantation window in the termination region. A constant-space floating guard ring (CS-FGR) was sensitive to the variation of the implantation window. A gradually increasing space (GIS) FGR was less sensitive to process deviations than the CS-FGR. We concluded that the GIS-FGR is sufficiently stable for use in high-voltage SiC devices at surface charge densities (Q_{surf}/q) of 0 to $-1 \times 10^{12} \text{ cm}^{-2}$ and implantation window variations of -0.3 to $+0.3 \mu\text{m}$. The optimized GIS-FGR exhibited a high breakdown voltage of over 8 kV at all the Q_{surf}/q values and in the implantation window variation range considered in this paper.

Index Terms—SiC, power device, Edge termination, JTE, FGR

I. INTRODUCTION

4H-Silicon carbide (SiC) has attracted attention as a

next-generation power semiconductor material owing to its wide band gap (3.26 eV), high critical electric field ($E_C = 3 \text{ MV/cm}$), and high thermal conductivity (4.9 W/cm \cdot °C). These properties make it suitable for high-power, high-frequency, and high-temperature operation. Moreover, the high E_C provides the significant advantages of a low on-resistance and excellent reverse blocking characteristics [1, 2].

Several edge termination structures for SiC power devices, such as the field plate [3, 4], floating guard ring (FGR) [5, 6], mesa-etched termination [7], and junction termination extension (JTE) [8-10], have been investigated by various groups. A reduction in breakdown voltage (BV) due to unexpected process conditions has been reported [11, 12]. To obtain stable blocking characteristics regardless of process deviations, new edge termination structures are necessary [13-16]. It is well known that the surface charge density (Q_{surf}/q) at the interface between SiC and a passivation layer affects the operation of power devices [17, 18]. Post-oxidation annealing in NO or N₂O ambient has been widely used to reduce Q_{surf}/q . In addition, it is a well-validated method of improving the channel mobility of n-channel SiC metal-oxide-semiconductor field-effect transistors [19-21]. In both the NO and N₂O processes, a negative surface charge density is formed on the n-type SiC surface [22]. The presence of the Q_{surf}/q affects the E-field distribution along the surface at the edge termination structures. The blocking characteristics of ultrahigh-voltage devices are strongly affected by the surface charge density because of the relatively low doping concentration in the drift layer and long termination length.

The JTE is typically used in power devices owing to

Manuscript received Nov. 27, 2020; reviewed Apr. 7, 2021; accepted Apr. 8, 2021

¹Department of Electrical Engineering, Pusan National University, Busan 46241, Korea

²Power Semiconductor Research Center, Korea Electrotechnology Research Institute, Changwon 51543, Korea

³School of Electronic Engineering, Kumoh National Institute of Technology, Gumi 39177, Korea

E-mail : ogseok@kumoh.ac.kr; hwkim@keri.re.kr

its simple design and processes. It exhibits a high BV when the implantation dose in the JTE region is close to the cross-sectional concentration in the drift layer [8, 9]. Although the ion implantation dose can be precisely controlled, the profiles of depletion regions in the drift layer are affected by the charge states at the SiC/passivation layer interface and by the activation efficiency of implanted ions [11, 23].

The FGR is also widely used as an edge termination structure because it effectively reduces E-field crowding [5, 24]. Also, gradually increasing ring-space structure for FGR was reported to obtain high breakdown voltage [25]. However, the design of FGR structures is complicated because various design and process parameters such as the ring space, ring width (W_{FGR}), doping concentration, and surface charge density should be considered. A narrow space is required near the main junction to transfer potential from anode to edge termination regions. In case of outer regions of termination, a relatively wide space is required for large potential drops to obtain uniform E-field distribution and high breakdown voltage. CS-FGR may not be suitable for uniform E-field distribution because of the constant value of spaces.

The ring spaces are affected by the conditions required for processes such as photolithography, hard mask etching, and high-temperature annealing to diffuse the implanted ions. For these reasons, the process conditions must be accurate and repeatable to provide a consistent ring space and blocking characteristics [26]. In addition, photoresist and hard mask layers have a non-perpendicular slope after patterning processes; consequently, the implantation window can differ from the intended pattern width at the photomask [27, 28]. Moreover, the width of the photoresist pattern may be also affected by the exposure time during photolithography processes [29]. Note that lateral straggling of implanted ions increases W_{FGR} by 0.2-0.3 μm , which considerably changes the depletion shape in the drift regions [30].

In this study, we investigated the BV characteristics of edge termination structures, including the JTE, constant space FGR (CS-FGR), and gradually increasing space FGR (GIS-FGR), with a focus on process deviations. The effects of Q_{surf}/q and the ring space variation on the BV were analyzed, and the electrical stability was evaluated.

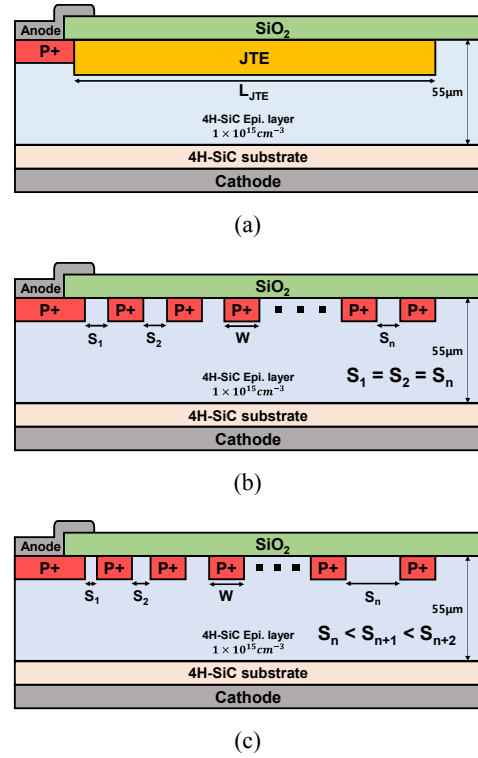


Fig. 1. Schematic illustrations of structures of (a) JTE, (b) CS-FGR, (c) GIS-FGR.

The BV of a proposed GIS-FGR is sufficiently stable for 6.5 kV SiC power devices against the Q_{surf}/q and ring space variation.

II. SIMULATION MODEL AND DEVICE STRUCTURE

Numerical device simulations were performed using the Silvaco TCAD simulator. The parallel electric-field dependence, Shockley-Read-Hall recombination, Auger recombination, and band gap narrowing models were used for breakdown analysis. The avalanche breakdown was simulated using the impact ionization model of Selberherr [31, 32]. Fig. 1 schematically illustrates the structures of the JTE, CS-FGR, and GIS-FGR. The thickness and doping concentration of the drift layer were 55 μm and $1 \times 10^{15} \text{ cm}^{-3}$, respectively. The simulated BV of the ideal parallel-plane junction with these parameters was 12.4 kV.

We assumed that a passivation layer is formed by the following processes: thermal oxidation of 50-nm-thick SiO₂, post-oxidation annealing in NO ambience, and deposition of 1- μm -thick SiO₂. The length and doping

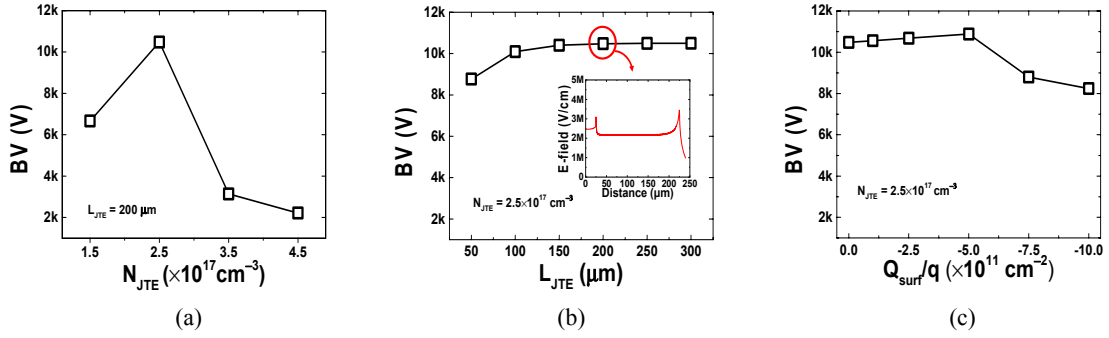


Fig. 2. Simulated BV for various values of JTE parameters (a) N_{JTE} , (b) L_{JTE} , (c) Q_{surf}/q .

concentration of the JTE ranged from 50 to 300 μm and 1.5×10^{17} to $4.5 \times 10^{17} \text{ cm}^{-3}$, respectively. Both the CS-FGR and GIS-FGR had 50 rings and a W_{FGR} value of 1.5 μm . The n_{th} ring space is determined using Eq. (1).

$$S_1 + (n-1)S_i = S_n \quad (1)$$

where S_1 is the first ring space, and S_i is the increment of the ring space for the GIS-FGR.

S_1 of the GIS-FGR was fixed at 1 μm . In addition, S_i was varied from 0.05 to 0.3 μm to analyze the blocking characteristics.

III. SIMULATION RESULTS AND DISCUSSION

Fig. 2(a) shows the BVs of JTEs with various doping concentrations (N_{JTE}) without considering surface charges. We obtained a maximum BV of 10,481 V at $N_{JTE} = 2.5 \times 10^{17} \text{ cm}^{-3}$. The BVs for various JTE lengths (L_{JTE}) are shown in Fig. 2(b), and the inset shows the E-field distribution for $L_{JTE} = 200 \mu\text{m}$. No significant improvement was observed at L_{JTE} values exceeding 200 μm . Fig. 2(c) shows the Q_{surf}/q dependence of the BV for $N_{JTE} = 2.5 \times 10^{17} \text{ cm}^{-3}$ and $L_{JTE} > 200 \mu\text{m}$. The BV changes when the Q_{surf}/q value on the SiC surface is negative because the surface charges affect the N_{JTE} value at the maximum BV.

Table 1-1 and 1-2 present the blocking characteristics of SiC devices using a JTE, including the average BV and its standard deviation against N_{JTE} and Q_{surf}/q variations, respectively. The JTE structure with $N_{JTE} = 2.5 \times 10^{17} \text{ cm}^{-3}$ and $L_{JTE} = 200 \mu\text{m}$ exhibited a high average BV of 10,040 V. The average BVs of the JTE structures with different N_{JTE} values are lower than those of the device with $N_{JTE} = 2.5 \times 10^{17} \text{ cm}^{-3}$. In addition, the

Table 1-1. Blocking characteristics of JTE in process deviations ($Q_{surf}/q = 0$ to $-1 \times 10^{12} \text{ cm}^{-2}$)

N_{JTE} (cm^{-3})	Average BV (V)	Standard deviation (%)
1.5×10^{17}	7030	5
2.5×10^{17}	10040	10
3.5×10^{17}	3250	3

Table 1-2. Blocking characteristics of JTE in process deviations ($N_{JTE} = 1.5 \times 10^{17}$ to $4.5 \times 10^{17} \text{ cm}^{-3}$)

Q_{surf}/q (cm^{-2})	Average BV (V)	Standard deviation (%)
0	5620	57
-1×10^{11}	5680	57
-5×10^{11}	5910	57
-1×10^{12}	5460	45

BVs of JTE structures with various N_{JTE} values showed very large standard deviations of 45-57%, indicating that the BV of the JTE structure depends strongly on N_{JTE} .

Fig. 3 shows the BVs of CS-FGR structures with ring spaces of 1.1 to 3.8 μm . For a ring space of 2 μm , the maximum BV was 6,840 V; the corresponding E-field distribution is shown in the inset. When the ring space is narrower or wider than 2 μm , the BV of the CS-FGR structures is much lower. The ring space can change not only during the patterning process but also during the implantation processes because lateral straggling of Al ions can result in a narrow ring space [13].

Fig. 4 shows the BV versus the ring space variation (-0.3 to $+0.3 \mu\text{m}$) at $Q_{surf}/q = 0, -1 \times 10^{11}, -5 \times 10^{11},$ and $-1 \times 10^{12} \text{ cm}^{-2}$. The ring space and Q_{surf}/q affect the BV because variation of these parameters changes the optimal point of space. However, the CS-FGR structures have a nonuniform E-field distribution, as shown in the inset, because a potential drop occurs along the CS-FGR structure.

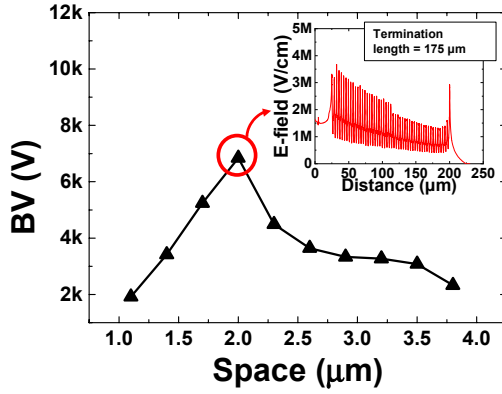
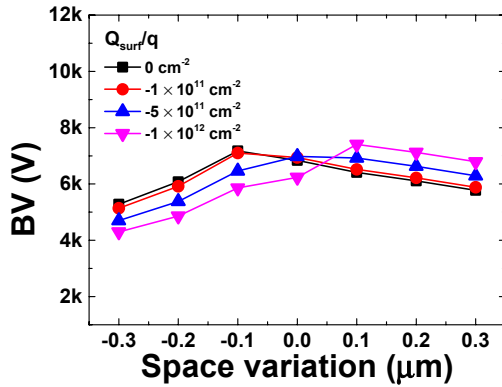


Fig. 3. BV of CS-FGR versus ring space.

Fig. 4. BV of CS-FGR versus ring space variation for various Q_{surf}/q .**Table 2-1.** Blocking characteristics of CS-FGR with process deviations (Space variation = -0.3 to +0.3 μm)

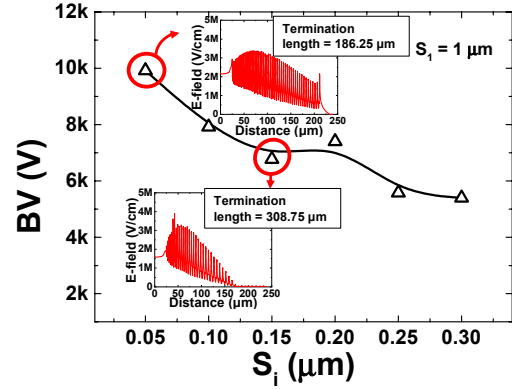
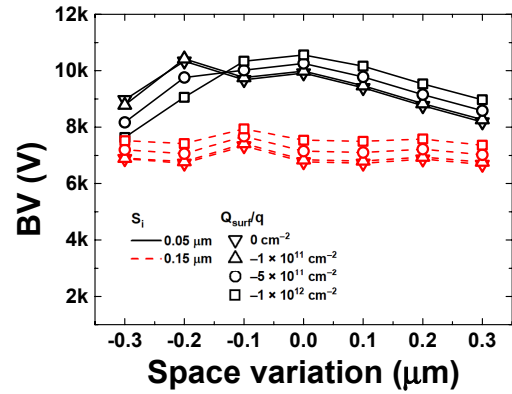
Q_{surf}/q (cm^{-2})	Average BV (V)	Standard deviation (%)
0	6256	8
-1×10^{11}	6264	9
-5×10^{11}	6163	13
-1×10^{12}	6106	18

Table 2-2. Blocking characteristics of CS-FGR with process deviations ($Q_{surf}/q = 0$ to $-1 \times 10^{12} \text{ cm}^{-2}$)

Space variation (μm)	Average BV (V)	Standard deviation (%)
-0.3	4854	7
0	6750	4
+0.3	6187	6

As shown in Table 2-1 and 2-2, the blocking characteristics of the CS-FGR structures may not provide the required BVs for 6.5 kV devices.

A ring space adjacent to the main junction must be narrow to deliver potential from the main junction to

Fig. 5. BV of GIS-FGR versus S_i .Fig. 6. BV of GIS-FGR versus ring space variation for various Q_{surf}/q , and S_i values.

edge termination structures. However, other spaces that are further from the main junction must be wide enough to afford an effective potential drop across the edge termination structures; consequently, a gradually increasing space can provide stable blocking characteristics [25]. Fig. 5 shows the BVs of simulated GIS-FGR structures with various S_i . The insets show the E-field distributions for $S_i = 0.05$ and $0.15 \mu\text{m}$. When $S_i = 0.15 \mu\text{m}$, the E-field is crowded in front of the GIS-FGR structure. The GIS-FGR with $S_i = 0.05 \mu\text{m}$ has a wide E-field distribution and high BV ($>10 \text{ kV}$).

Fig. 6 shows the BVs of GIS-FGR structures versus ring space variation for various Q_{surf}/q values. The GIS-FGR structure has an excellent E-field distribution even when the ring space is unintentionally varied during patterning. The BV for $S_i = 0.15 \mu\text{m}$ tends to increase for negative Q_{surf}/q values because for negative Q_{surf}/q , the depletion regions are extended along the surface [23]. By contrast, BV decreases when $S_i = 0.05 \mu\text{m}$ because the E-field is distributed uniformly; consequently, it is rather

Table 3-1. Blocking characteristics of GIS-FGR in process deviations (space variation = -0.3 to +0.3 μm)

S_i (μm)	Q_{surf}/q (cm ⁻²)	Average BV (V)	Standard deviation (%)
0.15	0	6850	3
	-1×10^{11}	6920	3
	-5×10^{11}	7220	2
	-1×10^{12}	7570	2
0.05	0	9480	7
	-1×10^{11}	9520	7
	-5×10^{11}	9550	7
	-1×10^{12}	9590	8

Table 3-2. Blocking characteristics of GIS-FGR in process deviations ($Q_{surf}/q = 0$ to -1×10^{11} cm⁻²)

S_i (μm)	Space variation (μm)	Average BV (V)	Standard deviation (%)
0.15	-0.3	7120	4
	0	7070	4
	+0.3	6950	4
0.05	-0.3	8390	6
	0	10180	2
	+0.3	8500	3

sensitive than that at $S_i = 0.15$ μm. For a large Q_{surf}/q and narrow ring space, the depletion regions exhibit rapid lateral expansion, and E-field crowding occurs at the end of the final ring.

Table 3-1 and 3-2 show the average and standard deviation of the BV of the GIS-FGR structures when $S_i = 0.05$ or 0.15 μm for Q_{surf}/q and ring space variations, respectively. We obtained fairly a small standard deviation of 2% against Q_{surf}/q variation from 0 to -1×10^{12} cm⁻². Despite the surface charge density and ring space variation, we obtained a high BV (>8 kV) for the GIS-FGR with $S_i = 0.05$ μm. We verified that the GIS-FGR is sufficiently stable for use in 6.5 kV SiC power devices despite process deviations during photolithography, etching, and ion implantation.

V. CONCLUSIONS

The effects of process deviations on the blocking characteristics of 6.5 kV SiC power devices were investigated to obtain devices that are unaffected by these variations. Simulations of a JTE structure showed that the standard deviation of the BV was 45-57% for various N_{JTE} values. Moreover, the presence of Q_{surf}/q changed

the optimal N_{JTE} value. A CS-FGR showed standard deviations of 4-18% and an average BV of 6,750 V owing to a nonuniform E-field. For a GIS-FGR with $S_i = 0.05$ μm, the standard deviation was 2-8%. In addition, we obtained a maximum average BV of 10,180 V, and a high BV (>8 kV) was obtained for various ring space variation and Q_{surf}/q values. Our results, including the electrical characteristics and validation of the effects of process deviations, provide stable blocking capability for 6.5 kV SiC power devices.

ACKNOWLEDGMENTS

This work was supported by the National Research Foundation of Korea (NRF) grant funded by the Korea government (MSIT) (No. 2021R1G1A1003487)

REFERENCES

- [1] O. Seok, et al, "Effects of junction profiles in bottom protection p-well on electrical characteristics of 1.2 kV SiC trench-gate MOSFETs," *Microelectron. Eng.*, Vol. 88, No. 3, pp. 111280, Dec., 2019.
- [2] O. Seok, et al, "Effects of trench profile and self-aligned ion implantation on electrical characteristics of 1.2 kV 4H-SiC trench MOSFETs using bottom protection p-well," *Jpn. J. Appl. Phys.*, Vol. 57, No. 6, pp. 06HC07, May, 2018.
- [3] F. Conti and M. Conti, "Surface Breakdown in Silicon Planar Diodes Equipped with Field Plate", *Solid-State Electronics*, vol. PS-15, pp. 93-105, Jan., 1972.
- [4] M. C. Tarplee, V.P. Madangarli, Quinchun Zhang and T.S. Sudarshan "Design rules for field plate edge termination in SiC Schottky diodes," *IEEE Trans. Electron Devices*, Vol. 48, No. 12, pp. 2659-2664, Dec., 2001.
- [5] K.- P. Brieger, W. Gerlach and J. Pelka, "Blocking capability of planar devices with field limiting rings," *Solid State Electronics*, Vol. 26, No. 8, pp. 739-745, Aug., 1983.
- [6] D. C. Sheridan, et al, "Design and fabrication of planar guard ring termination for high-voltage SiC diodes," *Solid-State Electronics*, Vol. 44, No. 8, pp. 1367-1372, Aug., 2000.

- [7] V. A. K. Temple and M.S. Adler, "Calculation of the diffusion curvature related avalanche breakdown in high-voltage planar p-n junctions," *IEEE Trans. Electron Devices*, Vol. 22, No. 10, pp. 910-916, Oct., 1975.
- [8] V. A. K. Temple, "Junction termination extension (JTE), A new technique for increasing avalanche breakdown voltage and controlling surface electric fields in P-N junctions," in *International Electron Devices Meeting, IEEE*, Dec., 1977.
- [9] D. C. Sheridan, et al, "Comparison and optimization of edge termination techniques for SiC power devices," In *Proceedings of the 1999 IEEE Int. Symp. Power Semiconductor Device and ICs*, 191, Osaka, Japan, June 2001.
- [10] V. A. K. Temple, "Increased Avalanche Breakdown Voltage and Controlled Surface Electric fields using a Junction Termination Extension (JTE)," *IEEE Trans. Electron Devices*, Vol. 30, pp. 954-957, Aug., 1983.
- [11] J. R. Trost, et al, "The effect of charge in junction termination extension passivation dielectrics," In *Proceedings of the 1999 IEEE Int. Symp. Power Semiconductor Device and ICs*, Toronto, Canada, May 1999.
- [12] R. Ghandi, et al, "Surface-Passivation Effects on the Performance of 4H-SiC BJTs," *IEEE Trans. Electron Devices*, Vol. 58, No. 1, pp. 259-265, Oct., 2010.
- [13] Y. F. Jiang, B. J. Baliga and A. Q. Huang "Influence of lateral straggling of implanted aluminum ions on high voltage 4H-SiC device edge termination design," *Mater. Sci. Forum*, Vol. 924, pp. 361-364, June, 2018.
- [14] W. Sung, E. V. Brunt, B. J. Baliga and Alex Q. Huang, "A New Edge Termination Technique for High-Voltage Devices in 4H-SiC-Multiple-Floating-Zone Junction Termination extension," *IEEE Electron Device Lett.*, Vol. 32, No. 7, pp. 880-882, May, 2011.
- [15] K. Kinoshita, T. Hatakeyama, O. Takikawa, A. Yahata and T. Shinohe, "A new termination structure providing stable and high breakdown voltages for SiC power devices," In *proceedings of the 2002 IEEE Int. Symp. Power Semiconductor Device and ICs*, New Mexico, USA, June, 2002.
- [16] W. Sung and B. J. Baliga, "A near ideal edge termination technique for 4500V 4H-SiC devices: The hybrid junction termination extension," *IEEE Electron Device Lett.*, Vol. 37, No. 12, pp. 1609-1612, Dec., 2016.
- [17] H. Yilmaz, "Optimization and surface charge sensitivity of high-voltage blocking structures with shallow junctions," *IEEE Trans. Electron Devices*, Vol. 38, No. 7, pp. 1666-1675, Jul., 1991.
- [18] J. Korec and R. Held, "Comparison of DMOS/IGBT-compatible high-voltage termination structure and passivation techniques," *IEEE Trans. Electron Devices*, Vol. 40, No. 10, pp. 1845-1854, Oct., 1993.
- [19] L. A. Lipkin, M. K. Das and J. W. Palmour, "N₂O Processing Improves the 4H-SiC:SiO₂ Interface," *Mater. Sci. Forum*, Vol. 389, pp. 985-988, Apr., 2002.
- [20] G. Y. Chung, et al, "Improved inversion channel mobility for 4H-SiC MOSFETs following high temperature anneals in nitric oxide," *IEEE Electron Device Lett.*, Vol. 22, No. 4, pp. 176-178, Apr., 2001.
- [21] H. F. Li, S. Dimitrijevic, H. B. Harrison and D. Sweatman, "Interfacial characteristics of N₂O and NO nitride SiO₂ grown on SiC by rapid thermal processing," *Appl. Phys. Lett.*, Vol. 70, No. 15, Feb., 1997.
- [22] T. Kimoto, et al, "Interface Properties of Metal-Oxide-Semiconductor Structures on 4H-SiC{0001} and (1120) Formed by N₂O Oxidation," *Jpn. J. Appl. Phys.*, Vol. 44, No. 3, pp. 1213-1218, Mar., 2005.
- [23] B. J. Baliga, *Fundamentals of Power Semiconductor Devices*; Springer: New York, USA, 2008.
- [24] T. Kimoto and J. A. Cooper, *Fundamentals of Silicon Carbide Technology*; Wiley: New York, USA, 2014.
- [25] W. Sung and B. J. Baliga, "A Comparative Study 4500-V Edge Termination Techniques for SiC Devices," *IEEE Trans. Electron Devices*, Vol. 64, No. 4, pp. 1647-1652, Feb., 2017.
- [26] H. Runhua, et al, "Development of 10 kV 4H-SiC JBS diode with FGR termination," *J. Semicond.*, Vol. 35, pp. 074005, Jul., 2018.
- [27] H. Runge, "Distribution of implanted ions under arbitrarily shaped mask edges," *Physica Status solidi (a)*, Vol. 39, pp. 595-599, Feb., 1977.

- [28] T. Sakurai, et al, "Lateral Spread of P⁺ Ions Implanted in Silicon through the SiO₂ Mask Window," *J. Appl. Phys.*, Vol. 59, pp. 1287-1290, Jul., 1979.
- [29] M. K. Jeffrey, et al, "A photolithographic method to create cellular micropatterns," *Biomaterials*, Vol. 27, No. 27, pp. 4755-4764, Sep., 2006.
- [30] J. Müting, et al, "Lateral straggling of implanted aluminum in 4H-SiC" *Appl. Phys. Lett.*, Vol. 116, No. 1, pp. 012101, Jan., 2020.
- [31] S. Selberherr Analysis and Simulation of Semiconductor Devices; Springer: New York, USA, 1984.
- [32] A. G. Chynoweth "Ionization Rates for Electrons and Holes in Silicon" *Phy. Rev.*, Vol. 109, No. 5, pp. 1537-1540, Mar., 1958.



Junki Jung received the B.S. degree (2019) from Gyeongsang National University. Since 2019, He has been in the M.S. degree course at Pusan National University, Korea. His research interests include wide bandgap power semiconductors, such

as SiC device



Ogyun Seok received the B.S. degree (2008) from Kookmin University, Seoul and Ph.D. degree (2013) in Department of Electrical and Computer Engineering from Seoul National University, Seoul, Korea. From 2013 to 2014, he was a

postdoctoral Researcher in Department of Electrical and Computer Engineering at the University of Illinois at Urbana-Champaign in USA. His researches at Seoul National University and University of Illinois at Urbana-Champaign were power GaN HEMTs and GaN MOS-HEMTs using high-k gate stacks and Au-free electrodes for CMOS compatible processes. He joined Power Semiconductor Research Center at Korea Electrotechnology Research Institute in Korea as Senior Researcher. He developed SiC power semiconductor devices including SiC planar MOSFET, SiC trench

MOSFET, SiC Schottky barrier diode and SiC trench diode. Since 2020, he has been with Kumoh National Institute of Technology, Gumi, Korea, where he is an Assistant Professor in School of Electronic Engineering. He has published 35 papers in international journals. His research interests include GaN, SiC, Diamond power transistors.

In Ho Kang received Ph.D. degree from the Department of Information and Communications in Gwangju Institute of Science and Technology in 2004, Korea. Since 2006, he has been a Principal Researcher in Power Semiconductor Research Center at Korea Electrotechnology Research Institute.

Hyoung Woo Kim received B.S., M.S. and Ph.D. degree from the Department of Electrical and Computer Engineering, Ajou University, Suwon, Korea in 1998, 2000 and 2018, respectively. He is currently technical leader of Power Semiconductor Research Center of Korea Electrotechnology Research Institute

Wook Bahng received Ph.D. degree (1997) in Material Science and Engineering from Seoul National University, Seoul, Korea. He was a visiting researcher Electro-technical Laboratory, Tsukuba, Japan from 1997 to 2000. Since 2000, he has been a Principal Researcher in Power Semiconductor Research Center at Korea Electrotechnology Research Institute. Now, he is a Director of the Research Center.

Hojun Lee received the Ph.D. degree from Seoul National University in 1996. Since 2001, he has been with Pusan National University, Korea, where he is professor in Department of Electrical Engineering. His research interests include wide bandgap power semiconductors and plasma system modeling & analysis, such as CCP and MICP.